Arch. Mech., 44, 3, pp. 313–329, Warszawa 1992

Profiles of stationary shock waves for hexagonal discrete velocity model with all triple collisions

T. PŁATKOWSKI (WARSZAWA)

STATIONARY SHOCK WAVE profiles are investigated for the hexagonal discrete velocity model with binary and all triple collisions. The singular points corresponding to equilibrium limit states are studied analytically in the phase space of the relevant dynamical systems. The influence of triple collisions on various macroscopic quantities which characterize the shock profiles is investigated. The infinite Mach number case is treated as well as the shock profiles with general equilibrium distributions, for various directions of the shock propagation on the plane. Local density and entropy profiles in the shock transition zone are studied. The influence of a class of higher order, quadruple collisions is also discussed.

1. Introduction

RECENT APPLICATIONS of the lattice gases theory Frisch et al. [6, 7] to various fluid dynamic problems raised the question of including higher than binary collisions into the kinetic description of the flows and studying their influence on the macroscopic characteristics of the flows, see e.g. BELLOMO, LONGO [1], CHAUVAT *et al.* [3], CORNILLE [4, 5], GATIGNOL [8, 9], HARRIS [10], PŁATKOWSKI [13].

The basic lattice model, which gives the correct Navier-Stokes equations in the hydrodynamic limit, is the hexagonal lattice gas model FRISCH *et al.* [6]. The discrete velocity counterpart is the plane six-velocity model (HARRIS [10]), which will be further called the hexagonal discrete model. In this model one can effectively study the influence of multiple collisions on the flows.

One of the most studied applications is the determination of the shock wave profile. The problems of the existence of shock wave solutions to the true Boltzmann equation for arbitrary Mach number and of the determination of exact shock profiles belong to the most challenging open problems in the mathematical kinetic theory of gases. In general only approximate solutions are known, except for weak shock waves.

On the other hand, in discrete kinetic theory, there are several particular models for which the exact shock wave solutions have been constructed, beginning with the Broadwell model (BROADWELL [2]).

Shock wave profiles for the discrete model with triple collisions have been discussed in GATIGNOL [8], BELLOMO, LONGO [1], either by taking into account only a class of the triple collisions or, numerically, by studying shock formation from the Riemann type initial data. Exact solutions having the form of solitons were studied in CORNILLE [4].

In this paper we find explicitly the profiles of the stationary shock waves taking into account the binary and all classes of triple collisions in the hexagonal model for various directions of the shock propagation on the plane. We also discuss the influence of a class of quadruple collisions on the macroscopic characteristics of the flow.

We consider two cases: the infinite Mach number shocks, and shocks joining general Maxwell equilibrium states. In the former case we find explicit exact solutions, by solving

a boundary value problem for one ODE, whereas in the latter case we solve a system of two ODE with singular points corresponding to the equilibria ahead of and behind the shock. To find the solutions, we study the character of the singular points in the relevant two-dimensional phase space of the problem.

We analyse the influence of triple collisions on the profiles of various macroscopic quantities in the shock transition zone, in particular on the density and entropy profiles, and on the existence of the stationary shock solutions for shocks propagating in different directions on the plane.

Finally we discuss the influence of a class of quadruple collisions (those in which the total precollisional microscopic momentum of the system of colliding particles is nonzero) on the macroscopic profiles.

In the following sections we define the model and formulate the shock problem, then we find shock solutions and discuss analytical and numerical results for various considered cases.

2. Formulation of the problem

We consider the hexagonal discrete model, i.e. the plane regular 6-velocity model gas of particles, which move on a plane $x0y$ with the admissible velocity vectors

$$u_i = c\cos\left[(i-1)\frac{\pi}{3}\right]e_x + c\sin\left[(i-1)\frac{\pi}{3}\right]e_y, \quad i = 1,\dots,6, \tag{2.1}$$

where $e_x = (1,0)$, $e_y = (0,1)$ are the unit vectors of the Cartesian coordinate system. We use the nondimensional variables, and normalize $c = |u_i| = 1$. Denote by

$$N_i = N_i(t,r), \quad t \in R_+, \quad r \in R^2, \quad i = 1,\dots,6 \tag{2.2}$$

the distribution functions of the particles, joined to the velocity vector u_i. The Boltzmann evolution equation for the distribution N_i can be written as

$$\frac{\partial N_i}{\partial t} + u_i\frac{\partial N_i}{\partial r} = Q_i(N), \tag{2.3}$$

where Q_i denotes the collision term for the particles i, $i = 1,\dots,6$.

The model has been applied by several authors for various fluid dynamical and statistical physics problems, see e.g. HARRIS [10, 11], GATIGNOL [8], LONGO, MONACO [12], BELLOMO, LONGO [1], CORNILLE [4].

In this paper we consider the general collision operator Q_i in which we take into account binary, all triple collisions and a class of nontrivial quadruple collisions. In the considered model there are three types of triple collisions. In the first one ("pseudotriple collisions"), one of the three colliding particles remains after the collision in its precollisional state (i.e. it does not change the velocity). Collisions of this type thus increase the rate of the binary collisions. In the second type ("true triple collisions"), all colliding particles have different precollisional velocities and change their velocities after the collision. In the third type of collisions (for simplicity we call them "halftriple collisions"), two of the three colliding particles have the same precollisional velocities and all the particles change their velocities after the collision.

As to the higher order collisions, we illustrate their influence by considering a nontrivial class of quadruple collisions, in which the total precollisional microscopic momentum of colliding particles is nonzero, and all particles change their velocities after the collision.

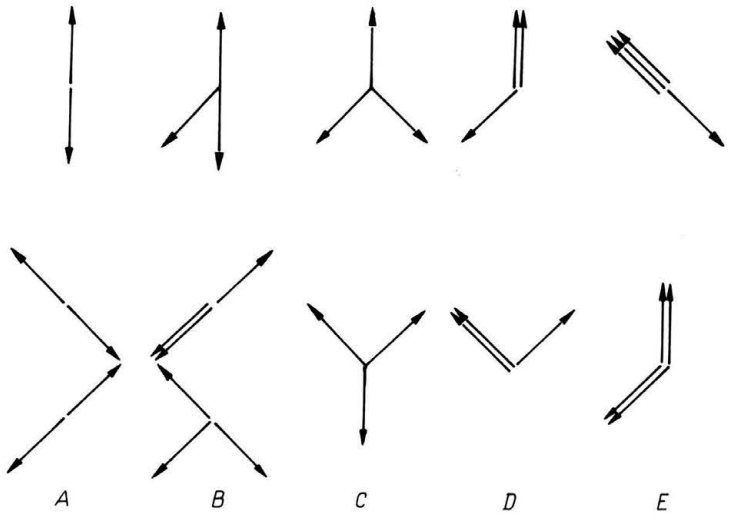

FIG. 1. Examples of binary and multiple collisions: a) binary, b) pseudotriple, c) true triple, d) halftriple, e) quadruple.

Examples of all types of collisions are visualized in Fig. 1, cf. also Appendix A for their contribution to the collision operators.

Denote by $\sigma_B, \sigma_P, \sigma_T, \sigma_H$ the cross-sections for the binary, pseudotriple, triple and halftriple collisions, respectively. The equation for N_1 reads

$$\begin{aligned}(2.4)\quad \frac{\partial N_1}{\partial t} + u_1 \frac{\partial N_1}{\partial r} &= \sigma_B(N_2N_5 + N_3N_6 - 2N_1N_4)\\ &+\sigma_P(N_1 + N_2 + N_3 + N_4 + N_5 + N_6)(N_2N_5 + N_3N_6 - 2N_1N_4)\\ &+\sigma_T(N_2N_4N_6 - N_1N_3N_5) + 2\sigma_H(N_2^2N_6 - N_1^2N_3) + 2\sigma_H(N_6^2N_2 - N_1^2N_5)\\ &+\sigma_H(N_2^2N_4 - N_3^2N_1) + \sigma_H(N_6^2N_4 - N_5^2N_1) + Q_M^1,\end{aligned}$$

where u_i are the velocity vectors of the particles with the distribution functions N_i, $r = (x, y)$ is the position vector in the $x0y$ plane. The collision operator Q_M^1 takes into account collisions of higher orders, cf. Appendix A. Analogous equations for $N_2, \ldots, N_6$ are also written in Appendix A.

3. Shock wave solutions

Our first objective is to investigate the existence of exact plane shock wave solutions. Then we study the corresponding density profiles and the dependence of the results on the direction of the shock wave propagation in the $x0y$ plane. We shall consider shock waves in two directions

$$(3.1)\qquad \text{direction } 1 : u_1, \quad \text{direction } 2 : u_1 + u_6.$$

3.1. Shock wave solutions in "u_1-direction"

In this section we consider solutions of (2.3) in the form of a stationary plane shock

wave, which propagates in the direction of the u_1-vector, i.e. we look for the wave solutions in the form

$$N_i(t, r) = N_i(z), \quad z = x + \beta t, \quad i = 1, \ldots, 6 \tag{3.2}$$

with the limiting values at $z \to \pm\infty$ corresponding to equilibrium states, see (3.7)–(3.9) below. With the symmetry relations

$$N_5(z) = N_3(z), \quad N_6(z) = N_2(z), \ \forall z \in R, \tag{3.3}$$

the initial system of six equations (cf. (2.4), and Appendix A) can be reduced to four ODE

$$\begin{aligned}
(\beta + 1)N_1' &= Q_B^* + Q_T + Q_H^1 + Q_M^1, \\
(\beta + 0.5)N_2' &= -\frac{1}{2}Q_B^* - Q_T + Q_H^2 + Q_M^2, \\
(\beta - 0.5)N_3' &= -\frac{1}{2}Q_B^* + Q_T + Q_H^3 + Q_M^3, \\
(\beta - 1)N_4' &= Q_B^* - Q_T + Q_H^4 + Q_M^4,
\end{aligned} \tag{3.4}$$

where

$$\begin{aligned}
Q_B^* &= Q_B + Q_P = (1 + 2\sigma_P N)(N_2N_3 - N_1N_4), \\
Q_T &= \sigma_T(N_2^2N_4 - N_3^2N_1), \\
N &= N_1 + 2N_2 + 2N_3 + N_4,
\end{aligned} \tag{3.5}$$

and Q_H^i, Q_M^i, $i = 1, \ldots, 4$ are defined in Appendix A. N is the (local) density of the gas, comma denotes the space derivative d/dz, and we have normalized $2\sigma_B$ to unity. The system (3.4) has two first integrals, corresponding to the mass conservation equation and the momentum conservation equation in the x-direction

$$\begin{aligned}
(\beta + 1)N_1 + (2\beta + 1)N_2 + (2\beta - 1)N_3 + (\beta - 1)N_4 &= C_1, \\
(\beta + 1)N_1 + (\beta + 0.5)N_2 - (\beta - 0.5)N_3 - (\beta - 1)N_4 &= C_2, \quad \forall z \in R,
\end{aligned} \tag{3.6}$$

where C_1, C_2 are arbitraty constants.

The shock wave problem consists in solving (3.4) for all $z \in R$ with the limit conditions at $\pm\infty$ corresponding to equilibrium states (Maxwellians).

We define the Maxwellians as the 4-coordinate vectors $m_1, \ldots, m_4$ such that for $N_1 = m_1$, the rhs in (3.4) vanish. It is easy to see that this occurs if

$$m_2m_3 = m_1m_4, \quad m_2^2m_4 = m_1m_3^2, \tag{3.7}$$

cf. the definitions of the multiple collision operators in Appendix A, with the symmetries (3.3).

Let us denote

$$\lim_{z \to -\infty} N_i(z) = m_i^-, \quad \lim_{z \to +\infty} N_i(z) = m_i^+, \quad i = 1, \ldots, 4. \tag{3.8}$$

In the following we assume for simplicity that

$$\lim_{z \to +\infty} N_i(z) = m, \quad i = 1, \ldots, 4, \tag{3.9}_1$$

where m is a given parameter (uniform distribution at $+\infty$).

The conservation equations (3.6) written at $\pm\infty$ give the Rankine–Hugoniot conditions, which relate the limit equilibrium states at $\pm\infty$ and the propagation speed β. In

our case

$$(3.9)_2 \quad \begin{aligned} &(\beta+1)m_1^- + (2\beta+1)m_2^- + (2\beta-1)m_3^- + (\beta-1)m_4^- = 6\beta m, \\ &(\beta+1)m_1^- + (\beta+0.5)m_2^- - (\beta-0.5)m_3^- - (\beta-1)m_4^- = 3\beta, \quad \forall z \in R. \end{aligned}$$

Further analysis depends substantially on the choice of the limit equilibrium states. We distinguish two cases.

3.1.1. Shock solutions for "cold" Maxwellian (Mach = $+\infty$). In this section we consider the case in which in one of the limit equilibrium states, all particles travel in the e_x direction. This case corresponds to the so-called infinite Mach number shock wave (BROADWELL [2]). We shall construct a unique (up to a translation in z, and normalization of m_1^-) shock wave solution of (3.4) for the infinite Mach number ("cold" Maxwellian at minus infinity), with the limit Maxwellians at $\pm\infty$ given by

$$(3.10) \qquad m_1^- = 1, \quad m_i^- = 0, \quad i = 2,3,4, \quad m_i^+ = m, \quad i = 1,2,3,4.$$

For simplicity we consider the case $Q_M^i = 0$, $i = 1,2,3,4$, i.e. solutions without quadruple collisions, but with all triple collisions taken into account. The quadruple collisions will be included in the next section, where we treat the general limit Maxwellian states.

Construction of the solution

From (3.9) and (3.10) we obtain $m = 0.5$, $\beta = 0.5$. It follows that $(3.4)_3$ becomes an algebraic relation

$$(3.11) \qquad 0 = -\frac{1}{2}Q_B^* + Q_T + Q_H^3,$$

(cf. Appendix A), from which we calculate N_3. For $\sigma_H = 0$

$$(3.12) \qquad N_3 = \frac{1}{2A}(-B + \sqrt{B^2 - 4AC}),$$

where

$$(3.13) \qquad A = 2(\sigma_T N_1 + 2\sigma_P N_2),$$

$$(3.14) \qquad B = N_2 + 2\sigma_P N_2(N_1 + 2N_2 + N_4) - 4\sigma_P N_1 N_4,$$

$$(3.15) \qquad C = -2\sigma_T N_2^2 N_4 - N_1 N_4 - 2\sigma_P N_1 N_4(N_1 + 2N_2 + N_4),$$

(we choose the positive sign in (3.12) to meet the positivity requirements for the distribution functions).

For $\sigma_H \neq 0$, N_3 is given by the roots of a polynomial of the third order, cf. Sec. 4 for a discussion of the uniqueness and positivity of the solution in that case. Then from the conservation equations (3.6) we calculate N_1, N_2, insert (3.12)–(3.15) into $(3.4)_4$ and solve the autonomous ODE for N_4. Once the solution is found, we obtain all the interesting macroscopic quantities of the flow, e.g. density, bulk velocity, entropy etc. Results will be discussed in Sec. 4.

REMARK

If we eliminate in (3.4) all the non-binary collisions except the pseudotriple ones, by setting $\sigma_T = \sigma_H = \sigma_M = 0$, then there are no shock solutions with the limit values (3.10). To see this, note that the system (3.4) has now three conservation equations (first integrals). Writing them at $\pm\infty$ with the relevant limit conditions, one can verify that the resulting system of three algebraic equations has no solutions. We omit details.

3.1.2. Shock solutions for "warm" Maxwellians. In the case of the infinite Mach number shock considered above, the problem has been reduced to one ODE, due to the particular value of the shock propagation. In this section we consider the general equilibrium state in front of the shock ("warm Maxwellians"). Due to (3.7), the general equilibrium distribution function depends on two arbitrary parameters. For convenience we choose the following general equilibrium distribution function in front of the shock

$$m_1^- = ay^2, \quad m_2^- = ay, \quad m_3^- = ay^{-1}, \quad m_4^- = ay^{-2}, \quad a, y \neq 0, \tag{3.16}$$

where a and y are arbitrary parameters (note that the conditions (3.7) for equilibria are satisfied identically). We prove

LEMMA

There exists a unique solution of the Rankine–Hugoniot equations $(3.9)_1$, $(3.9)_2$ for any given shock speed from the intervals

$$\beta \in \left(-1, -\frac{1}{2}\right) \cup \left(\frac{1}{2}, 1\right) \tag{3.17}$$

and the uniform Maxwellian state at plus infinity $m_i^+ = m$, $i = 1, \ldots, 4$. The parameters a and y are given by

$$y = \frac{(1-\beta)(2\beta+1)}{(1+\beta)(2\beta-1)}, \tag{3.18}$$

$$a = \frac{6\beta m y^2}{(\beta+1)y^4 + (2\beta+1)y^3 + (2\beta-1)y + \beta - 1}, \tag{3.19}$$

and are positive.

Proof

From $(3.9)_1$, $(3.9)_2$, (3.16) we obtain

$$(2\beta-1)(\beta+1)y^4 + (\beta-1)(2\beta+1)y^3 - (\beta+1)(2\beta-1)y + (2\beta+1)(1-\beta) = 0. \tag{3.20}$$

Due to the particular structure of the coefficients we find the 3-rd order root $y = 1$, leading to the same Maxwellians at $\mp\infty$ (i.e. no shock solution). The fourth root is given by (3.18). Expression for a is then obtained from $(3.9)_2$. Positivity of y and a holds in range of the shock speed values defined by (3.17), as can be easily seen by inspection. Note the singularities at $\beta = \mp 0.5$ in (3.18), (3.16), which correspond to the "cold" Maxwellian case considered previously.

Construction of the solution

From the conservation equations $(3.6)_{1,2}$ we calculate

$$N_3 = \frac{b_1 + b_2}{\beta - 0.5}, \quad N_4 = \frac{b_1 + 2b_2}{1-\beta} \tag{3.21}$$

with

$$\begin{aligned} b_1 &= C_1 - (\beta+1)N_1 - (2\beta+1)N_2, \\ b_2 &= C_2 - (\beta+1)N_1 - (\beta+0.5)N_2, \end{aligned} \tag{3.22}$$

where C_i are uniquely determined from the Maxwellian at $+\infty$; then we insert (3.21) into $(3.4)_{1,2}$.

Now the shock problem can be formulated as follows. We look for the positive solutions of the system of two ODE

$$N_1' = \frac{Q_B^* + Q_T + Q_H^1 + Q_M^1}{\beta + 1},$$
$$N_2' = -\frac{\frac{1}{2}Q_B^* + Q_T - Q_H^2 - Q_M^2}{\beta + 0.5}, \tag{3.23}$$

with the limit conditions

$$\lim_{z \to \pm\infty} N_i = M_i^{\mp}, \quad i = 1, 2, \tag{3.24}$$

where $m_i^+ = m$ is a given positive number (scaling parameter), β is a given free parameter, and m_i^-, $i = 1, 2$ are defined by (3.16), (3.18), (3.19). Thus the problem has been reduced to the solution of the dynamical system (3.23) with the limit conditions (3.24).

Note that on the phase plane (N_1, N_2) the points (m_1^-, m_2^-) and (m_1^+, m_2^+) are singular points of the system (3.23). We look for an integral curve of (3.23) joining these points.

An additional information on the solutions can be provided by analysis of the character of the singularities. Let N_i^0, $i = 1, \ldots, 4$, be an arbitrary Maxwellian. Linearizing $(3.23)_{1,2}$ around $N_i^0 : N_i = N_i^0 + n_i$, $i = 1, \ldots, 4$, we obtain the linear system

$$\frac{dn_1}{dz} = b_{11}n_1 + b_{12}n_2,$$
$$\frac{dn_2}{dz} = b_{21}n_1 + b_{22}n_2, \tag{3.25}$$

where the coefficients b_{ij} depend on the actual Maxwellian N_i^0, $i = 1, \ldots, 4$, and on σ_P, σ_T, σ_H, σ_M, β, m. Their explicit values are given in Appendix B.

The eigenvalues $\lambda_{1,2}$ of the matrix $[b_{ij}]$ determine the character of singularities of the equilibria. Their values are essential for the shock curve existence problem as well as for numerical calculations. In the numerical calculations we start in the direction determined by the relevant eigenvalue of the saddle, cf. Sec. 4 for more details.

Once N_1, N_2 are known, we calculate all the interesting macroscopic quantities. Results are discussed in Sec. 4.

3.2. Shock wave solutions in $u_1 + u_6$-direction

In this section we consider solutions of (2.3) in the form of a stationary plane shock wave, which propagates in the direction of the $u_1 + u_6$-vector, cf. (2.1). For simplicity of notation we turn the coordinate system so that this direction coincides with the x-axis, thus the particles u_1 now move in the direction

$$\cos\left(\frac{\pi}{6}\right)e_x + \sin\left(\frac{\pi}{6}\right)e_y. \tag{3.26}$$

We look for solutions of (2.3) in the form

$$N_i(t, r) = N_i(z), \quad z = x + \beta t, \quad i = 1, \ldots, 6 \tag{3.27}$$

with the symmetry relations

$$N_6(z) = N_1(z), \quad N_5(z) = N_2(z), \quad N_4(z) = N_3(z), \quad \forall z \in R, \tag{3.28}$$

which reduce (2.3) to a system of three equations

$$(\beta + q)N_1' = Q, \quad \beta N_2' = -2Q, \quad (\beta - q)N_3' = Q, \tag{3.29}$$

where

$$Q = (0.5 + \sigma_P N + \sigma_H(N_1 + N_3))(N_2^2 - N_3 N_1), \quad N = 2(N_1 + N_2 + N_3)$$

is the local density of the gas, $' = d/dz$, $q = \sqrt{3}/2$ and we use the same normalization of the binary collision cross-section as in the previously considered case.

Note that, due to (3.28), the problem actually has been reduced to that with the binary collisions, with the collision rate depending on the local state of the gas. The system (3.29) has two first integrals

$$\begin{aligned} 2(\beta + q)N_1(z) + \beta N_2(z) &= C_1, \\ (\beta + q)N_1(z) - (\beta - q)N_3(z) &= C_2, \quad \forall z \in R. \end{aligned} \tag{3.30}$$

As in Section 3.1 we discuss two cases.

1. Infinite Mach number shock

The limit "cold" Maxwellian at minus infinity is defined by $m_1^- = 1$ (normalization), $m_i^- = 0$, $i = 2, 3$, whereas at plus infinity we choose the uniform Maxwellian $m_i^+ = m$, $i = 1, 2, 3$. From the first integrals written at $\pm\infty$ we obtain $\beta = \sqrt{3}/3$, $m = 5/6$. With (3.30), the system (3.29) is reduced to one equation

$$N_1' = \frac{1}{\beta + q}(0.5 + \sigma_P N + \sigma_H(N_1 + N_3))(N_2^2 - N_3 N_1), \tag{3.31}$$

with the limit conditions

$$\lim_{z \to -\infty} N_1(z) = m_1^- = 1, \quad \lim_{z \to +\infty} N_1(z) = m_1^+ = m, \tag{3.32}$$

where N_2, N_3 are calculated from (3.30) with $C_1 = 2(\beta + q)$, $c_2 = \beta + q$. Solution of (3.31) gives the exact density profile N and other macroscopic quantities, see Sec. 4.

2. General ("warm") Maxwellian at $-\infty$, uniform distribution at $+\infty$

The limit conditions for (3.31) are now

$$\lim_{z \to -\infty} N_i(z) = m_i^-, \quad (m_2^-)^2 = m_1^- m_2^-, \quad \lim_{z \to +\infty} N_i(z) = m, \quad i = 1, \ldots, 3. \tag{3.33}$$

The first integrals (3.30) written at $\mp\infty$ give two relations between the unknown constants. Thus, with the normalization $m = 1$ we obtain

$$\begin{aligned} m_2^- &= \frac{2\beta(C_1 - C_2) \mp \sqrt{\Delta}}{8 - 6\beta^2}, \quad \Delta = \beta^2(C_1 + C_3)^2 - 4C_1C_3(4 - 3\beta^2), \\ m_1^- &= \frac{C_1 - \beta m_2}{2(\beta + q)}, \quad m_3^- = \frac{C_1 - \beta m_2 - 2C_2}{2(\beta - q)}, \end{aligned} \tag{3.34}$$

where $C_1 = 3\beta + 4q$, $C_2 = 4q$, $q = \sqrt{3}/2$, and the shock speed β is a free parameter. We solve again (3.31) with the proper limit conditions for N_1. Results will be discussed in the next Section.

4. Results

In the case of the infinite Mach number shock, we solve one ODE, $(3.4)_4$ with N_1, N_2 defined by (3.15), and N_3 defined by (3.12)–(3.16) for $\sigma_H = 0$, and by the roots of the relevant polynomial of the third order for $\sigma_H \neq 0$. In the calculations we checked that in all the cases considered there is exactly one positive root of (3.12) for $\sigma_H = 0$, and of the relevant polynomial of the third order for $\sigma_H \neq 0$.

In the case of "warm" Maxwellians, we solve $(3.23)_{1\text{-}2}$ with the initial data $N_i(0) = m_i^- + \varepsilon_i$ or $N_i(0) = m_i^+ + \varepsilon_i, i = 1, 2$, depending on the character of the singular points. The differential equations are solved numerically using the standard Runge–Kutta's IV-th order procedure. The initial direction of the integral curve is calculated from the analysis of the relevant saddle singular point. The distance between the initial starting point and the saddle was of order $\varepsilon = 10^{-8}$ and the results were quantitatively the same as if ε was changed by several orders of magnitude. The step of integration was of order 10^{-2}.

The shock curve is defined as the integral curve which joins the two singular points corresponding to the equilibria ahead and behind the shock. Once the shock curve has been found, we calculate all the interesting macroscopic characteristics of the flow. In particular we define local bulk velocity, and local entropy, respectively, by

$$U = \frac{1}{N}\sum_{i=1}^{6} N_i u_i, \qquad E = -\sum_{i=1}^{6} N_i \ln N_i, \tag{4.1}$$

where $N = \sum_{i=1}^{6} N_i$ is the local density of the gas.

Below we discuss the results for various considered cases. The relevant macroscopic quantities are normalized so that their equilibrium values in front and behind the shock are respectively 0 and 1. In Subsecs. 1, 2, 3 we discuss the profiles with binary and triple collisions, in Subsec. 4 we discuss the influence of higher order collisions.

4.1. Infinite Mach number shock, u_1 direction (Sec. 3.1.1.)

As expected from the considerations of the previous Section, the shock density profiles depend heavily on the numerical values of the triple collision cross-sections and become infinitely thick for $\sigma_T^2 + \sigma_H^2 \to 0$ (i.e. there is no infinite Mach number shock in this direction, cf. Remark in Sec. 2. For increasing values of the triple collision cross-sections, the shock thickness decreases; the triple collisions speed up the process of equilibration. We note, however, that the influence of the various types of triple collisions on the density shock structure is different, cf. Fig. 2.

In Fig. 2 we plotted infinite Mach number shock profiles for different values of the cross-section for triple collisions. The steepest profile corresponds to the largest considered values, i.e. 10^{-1}, cf. the curve A, the opposite case corresponds to all the cross-sections equal to 10^{-2}, cf. curve B, the long relaxation tail due to the slower energy exchange through triple collisions.

In order to compare the influence of the various types of triple collisions, we also plotted the density profiles in the cases in which one of the cross-sections is by two orders of magnitude smaller than the two others, cf. the curve C, D, E. Taking A as a reference profile, we note that the absence of halftriple collisions changes this profile more than the absence of pseudotriple ones, as can be seen by comparison of the curves C, E. The absence of true triple collisions does not cause any pronounced changes in the profiles, cf. the curves A, D.

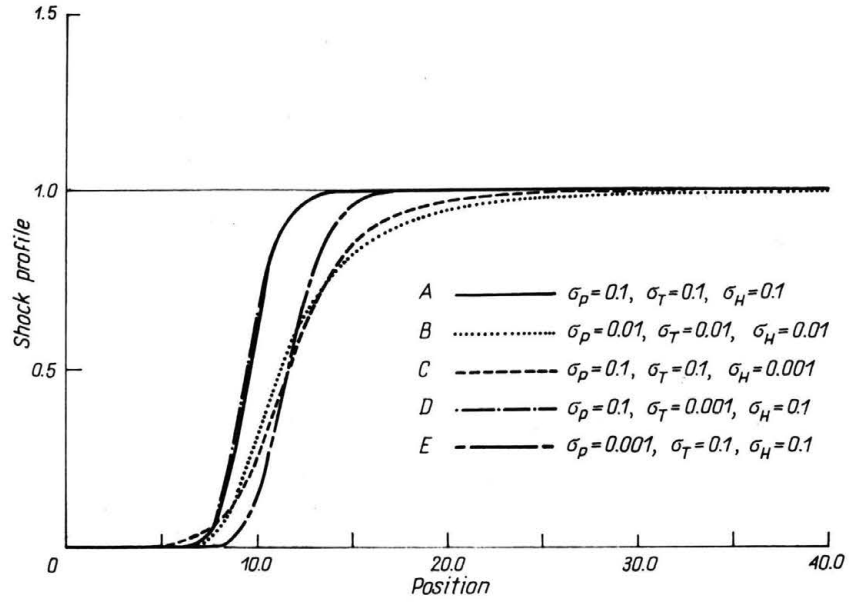

FIG. 2. Shock density profiles, „cold" Maxwellian, e_x-direction.

We also note an asymmetry of the considered density profiles with respect to the "classical" hyperbolic tangent profiles. The asymmetry becomes more pronounced for decreasing values of the cross-sections.

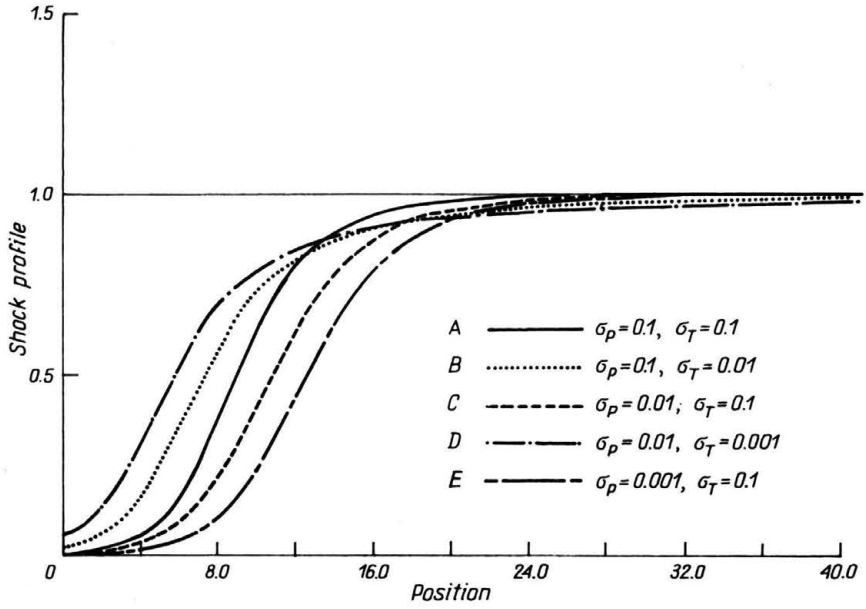

FIG. 3. Shock density profiles, „cold" Maxwellian, $\sigma_H = 0$, e_x-direction.

In Fig. 3 we discuss for comparison the case without halftriple collisions ($\sigma_H = 0$). Note the larger relaxation tails as compared to the previous case with the halftriple collisions present. In particular, for $\sigma_P = 0.1, \sigma_T = 0.01$ (case B) we obtain a long relaxation tail on the density profile, resulting from the smaller collision rate for true triple collisions; more collisions are needed to reach equilibrium than in the "reference case" $\sigma_P = 0.1$, $\sigma_T = 0.1$.

For comparison we also plotted in Fig. 3 the shock profiles for $\sigma_P = 0.01$, $\sigma_T = 0.1$, and $\sigma_P = 0.001$, $\sigma_T = 0.1$, cf. the curves C, E. The absence of true triple collisions results in longer relaxation tails than the absence of pseudotriple ones.

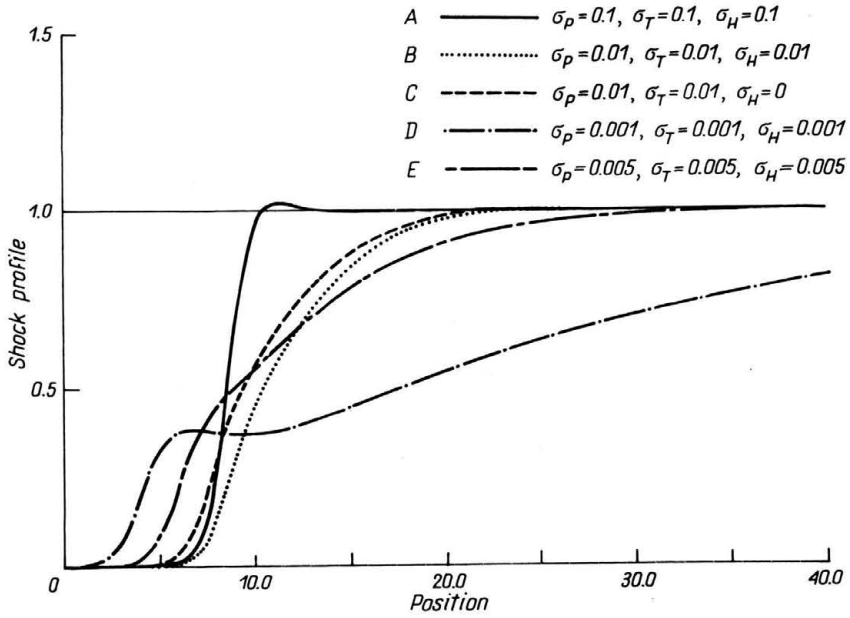

FIG. 4. Entropy profiles in the shock, „cold" Maxwellian, e_x-direction.

Another interesting quantity is the local entropy, cf. (4.1). Its changes in the shock zone are shown in Fig. 4 for specific values of the collision cross-sections. We note several interesting features of the profiles: entropy overshoot for "large" (10^{-1}) values of the cross-sections, cf. the curve A, and an undershoot accompanied by a long equilibration tail for all the cross-sections equal to (10^{-3}), cf. the curve D. Other intermediate values of the cross-sections also lead to "nonstandard" profiles, the curves B, E, cf. also [14].

4.2. Shocks for "warm" Maxwellians, u_1-direction (Sec. 3.1.2)

In this case numerical results depend not only on the cross-sections for the triple collisions, but also on the shock speed β, as will be discussed below.

In Fig. 5 we plot shock profiles for $\beta = 0.55$ for various cross-sections. We note similar phenomena as in the case of the infinite Mach number. Taking the case without the triple collisions as the reference one, cf. the curve A, we note that the profiles become steeper for increasing values of the cross-sections. A small "amount" of the triple collisions results in appearance of the relaxation tail, cf. curve B. Comparison of the curves C and D shows

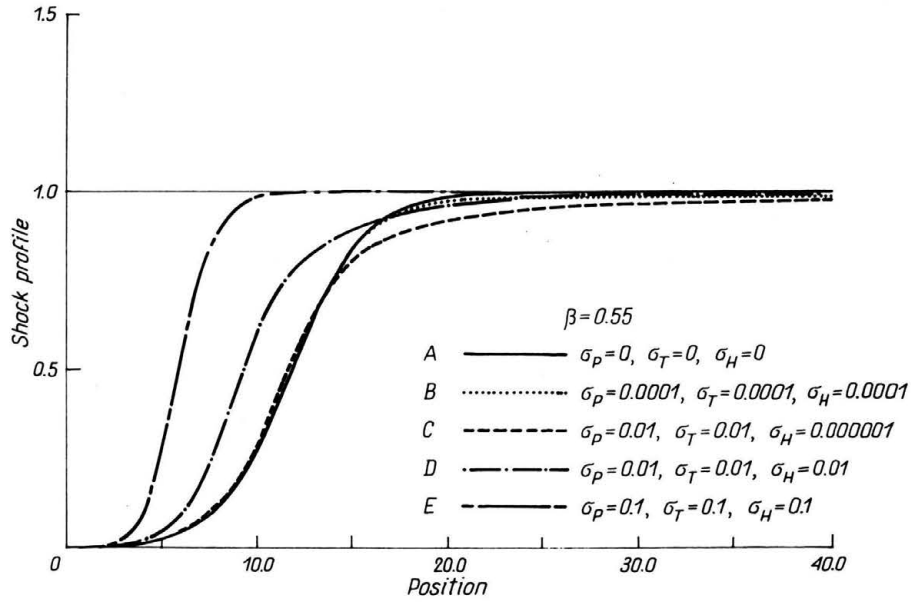

FIG. 5. Shock density profiles, „warm" Maxwellian, $\beta = 0.55, e_x$-direction.

the influence of halftriple collisions on the equilibration speed; their presence diminishes the relaxation tails. The steepest considered profiles correspond to all cross-sections equal to 10^{-1}.

As expected, the shock thickness depends heavily on the shock speed, and for $\beta = \sqrt{2}/2$ (sound speed) it becomes infinite.

In Fig. 6 we compare the density profiles for the case in which only one type of the triple collisions is present. For simplicity we assume that the relevant cross-sections have the same value 0.1. The shock speed is $\beta = 0.68$. Figure 6 shows that the presence of the pseudotriple collisions influence the reference binary collision profile, cf. the curve A, more than the halftriple ones, the halftriple—more than the true triple ones.

In Fig. 7 we show the influence of different types of collisions for $\beta = 0.52$. Similar phenomena were found for other values of the cross-sections and the propagation speeds.

4.3. Shock solutions for $u_1 + u_6$-direction (Sec. 3.2)

In general the results are similar to those for the case with only binary collisions. The main difference is that the total collision cross-section depends now on the local state of gas.

In this case the density profiles depend on the cross-sections σ_P, σ_H. Increasing these parameters, we obtain steeper shock profiles due to faster energy exchange inside the shock, as in the previously considered cases. The shock thickness is smaller than that for the u_1-direction.

The profiles being steeper for larger values of the cross-sections, the dependence on the cross-sections is not so big as for the previously considered u_1-dicretion, and the relaxation tails are less pronounced.

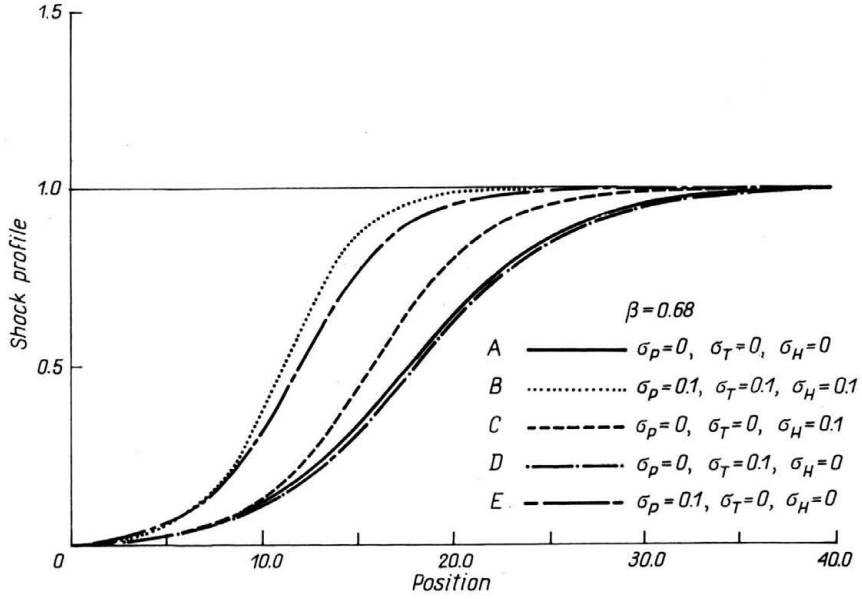

FIG. 6. Shock density profiles, „warm" Maxwellian, $\beta = 0.68$, e_x-direction.

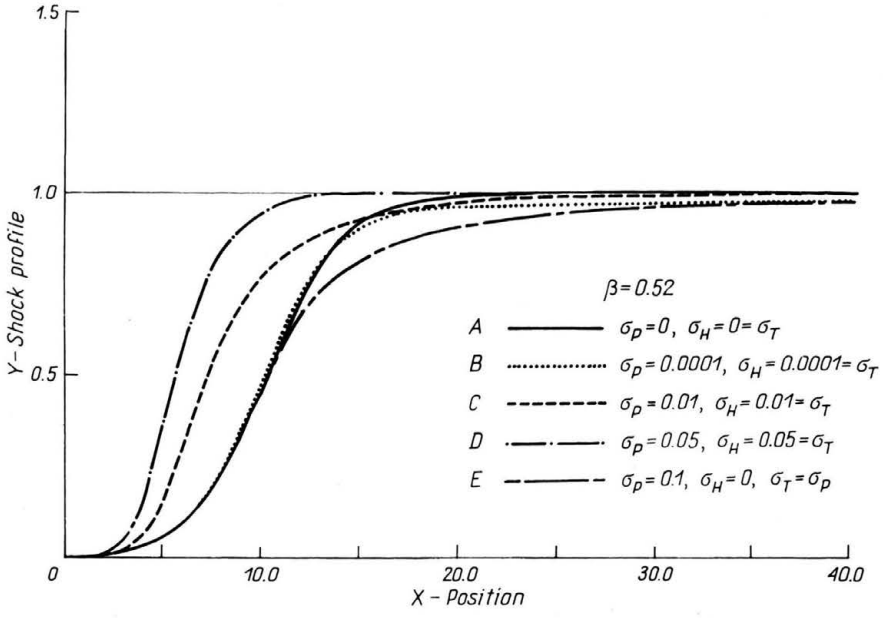

FIG. 7. Shock density profiles, „warm" Maxwellian, $\beta = 0.52$, e_x-direction.

As in the pure binary collisions case, we also found non-monotonic behaviour of the local entropy profiles, cf. CORNILLE [4], PŁATKOWSKI [14]. All these phenomena were found in the case of the "warm" Maxwellians as well as for the infinite Mach number. We omit the details.

4.4. Influence of quadruple collisions on the shock solutions; example

As an example of the changes which occur if we take into account higher order collisions we considered the influence of a class of quadruple collisions in which the total precollisional microscopic momentum of the system of the colliding particles is nonzero, and all particles change their postcollisional velocities, cf. Fig. 1. The corresponding collision operators are defined in Appendix A. Calculations indicate that the influence of these collisions on the shock profiles with binary and triple collisions is in general less pronounced than the influence of the triple collisions on the profiles in which only the binary collisions were taken into account. One can similarly include other classes of quadruple and higher order collisions.

5. Conclusions

In this paper we solved the shock wave problem for the hexagonal six-velocity model with binary and all triple collisions. We also investigated the influence of a class of quadruple collisions on the shock profiles for different values of the relevant cross-sections. In the considered model, there are several interesting features of the shock solutions, which we summarize here.

1. Nonsymmetrical density profiles.
2. Long equilibration tails for "small amount" of the triple collisions.
3. Different impacts of various classes of multiple collisions on the structure of the shock wave profiles.
4. Dependence of the results (e.g. of the shock thickness) on the direction of the shock propagation on the plane.

We note that the relaxation tails which appear if the triple collisions are taken into account, are similar to those which appear in other physically interesting cases of the shock profiles for the polyatomic gases, and for the mixtures of gases with very different molecular masses (disparate gas mixtures). In the former case the tails result from the difficult transfer of energy between translational and internal degrees of freedom, while in the latter case they result from the slow energy transfer in the collisions between the particles of different gases.

In the present model the possible explanation comes from the number of the collision invariants for the collision operator with binary collisions only (three linearly independent collision invariants), and that with the triple collisions taken into account (two collision invariants, corresponding to the conservation of mass and energy). The additional (spurious) collision invariant nullifies the binary collision operator, but not the sum of the binary and triple collision operators, see e.g. GATIGNOL [8, 9]. The terms which remain on the rhs can be interpreted as the source terms for the individual density distribution functions, similarly as the terms coming from the cross-collisions in the equations for the macroscopic variables describing the individual gas in the mixture of different gases.

Moreover, the Maxwellian distribution functions for the binary collision operator are different from those which take into account the binary and higher order collisions, cf. the expression (3.7) in the text. For small triple collision cross-sections the steep part of the profile corresponds to the binary collisions only, with the relevant Rankine–Hugoniot conditions, whereas the ultimate equilibrium state on the other side of the shock imposes the further relaxation, with the rate depending on the triple and higher order collision

cross-sections. If their values are comparable to the binary collision cross-section, both types of collisions equally influence the profile in the whole transition zone. The profiles become steeper due to the faster energy exchange, and the relaxation tails are not present.

The confirmation of such a point of view has been recently found by studying the family of models in which the number of the collision invariants corresponds to the number of the physical conservation laws of mass, momentum and energy, and the multiple collisions do not change the Maxwellian states CORNILLE, PŁATKOWSKI [5], PŁATKOWSKI [15]. It turns out that for such models the relaxation tails do not exist.

The results obtained in this paper also indicate that quantitative results for the flows described by models with higher order collisions may be rather sensitive to the actual values of the relevant collision cross-sections in the highly nonequilibrium regimes, and one must be careful in modelling the relevant collision terms.

One can also consider shock waves which propagate in any direction in the $x0y$ plane. In the general case, there exist three nontrivial conservation equations, and the initial system of six differential equations can be reduced to three autonomous equations ODE. The problem is then reduced to finding an integral curve of this system in a three-dimensional phase space, which joins two singular points, corresponding to equilibrium states in front and behind the shock. Our choice of the directions of the shock propagation, together with appropriate symmetry conditions, reduced the dimension of the problem by at least one, and provided a way to a more systematic analysis of the problem in the relevant phase space.

Appendix A

Below we give the evolution equations (2.4) for the remaining distribution functions of the hexagonal model with the binary and the higher order collisions.

$$(A.1)\quad \frac{\partial N_2}{\partial T} + u_2\frac{\partial N_2}{\partial r} = \sigma_B(N_1N_4 + N_3N_6 - 2N_2N_5) + \sigma_P N(N_1N_4 + N_3N_6 - 2N_2N_5) + \sigma_T(-N_2N_4N_6 + N_1N_3N_5) + 2\sigma_H(-N_2^2N_6 + N_1^2N_3) + \sigma_H(-N_6^2N_2 + N_1^2N_5) + 2\sigma_H(-N_2^2N_4 + N_3^2N_1) + \sigma_H(N_3^2N_5 - N_4^2N_2) + Q_M^2,$$

$$(A.2)\quad \frac{\partial N_3}{\partial t} + u_3\frac{\partial N_3}{\partial r} = \sigma_B(N_2N_5 + N_1N_4 - 2N_3N_6) + \sigma_P N(N_2N_5 + N_1N_4 - 2N_3N_6) + \sigma_T(N_2N_4N_6 - N_1N_3N_5) + \sigma_H(N_2^2N_6 - N_1^2N_3) + 2\sigma_H(N_4^2N_2 - N_3^2N_5) + 2\sigma_H(N_2^2N_4 - N_3^2N_1) + \sigma_H(N_4^2N_6 - N_5^2N_3) + Q_M^3,$$

$$(A.3)\quad \frac{\partial N_4}{\partial t} + u_4\frac{\partial N_4}{\partial r} = \sigma_B(N_2N_5 + N_3N_6 - 2N_1N_4) + \sigma_P N(N_2N_5 + N_3N_6 - 2N_1N_4) + \sigma_T(-N_2N_4N_6 + N_1N_3N_5) + 2\sigma_H(N_3^2N_5 - N_4^2N_2) + 2\sigma_H(N_5^2N_3 - N_4^2N_6) + \sigma_H(-N_2^2N_4 + N_3^2N_1) + \sigma_H(-N_6^2N_4 + N_5^2N_1) + Q_M^4,$$

where $N = N_1 + N_2 + N_3 + N_4 + N_5 + N_6$, Q_M^i take into account the collisions of the higher order. Analogous equations for N_5, N_6 are omitted due to the considered symmetries. We give the analytical structure of Q_M^i for the class of quadruple collisions, for which the total precollisional microscopic momentum of the system of the colliding particles is nonzero, and all particles change their postcollisional velocities, see Fig. 1.

$$(A.4) \qquad Q_M^1 = 2A - 3B - D + 2F, \qquad Q_M^2 = -3A + 2B + 2C - E,$$

$$(A.5) \qquad Q_M^3 = 2A - 3C + 2D - F, \qquad Q_M^4 = -B + 2C - 3D + 2E,$$

$$(A.6) \qquad Q_M^5 = -A + 2D - 3E + 2F, \qquad Q_M^6 = 2B - C + 2E - 3F,$$

where

$$(A.7) \qquad A = \sigma_M(N_2^3 N_5 - N_1^2 N_3^2), \qquad B = \sigma_M(N_1^3 N_4 - N_2^2 N_6^2),$$

$$(A.8) \qquad C = \sigma_M(N_3^3 N_6 - N_2^2 N_4^2), \qquad D = \sigma_M(N_4^3 N_1 - N_3^2 N_5^2),$$

$$(A.9) \qquad E = \sigma_M(N_5^3 N_2 - N_4^2 N_6^2) = C, \qquad F = \sigma_M(N_6^3 N_3 - N_1^2 N_5^2) = A.$$

With symmetries (3.3), the halftriple collision operators in (3.4), (3.11) in the main text are defined by

$$(A.10) \qquad Q_H^1 = 2H - 4G, \qquad Q_H^2 = -2H + 3G + I,$$

$$(A.11) \qquad Q_H^3 = 2H - G - I, \qquad Q_H^4 = -2H + 4I,$$

where

$$(A.12) \quad G = \sigma_H(N_1^2 N_3 - N_2^3), \quad H = \sigma_H(N_2^2 N_4 - N_3^2 N_1), \quad I = \sigma_H(N_3^3 - N_4^2 N_2).$$

Similar simplifications occur for Q_M^i, $i = 1, \ldots, 4$.

Appendix B

Coefficients of the matrix of the linearized system (3.25) are

$$(B.1) \qquad \begin{aligned} b_{11} &= f_{11} + f_{13}e_{11} + f_{14}e_{12}, \\ b_{12} &= f_{12} + f_{13}e_{12} + f_{14}e_{22}, \\ b_{21} &= f_{21} + f_{23}e_{11} + f_{24}e_{21}, \\ b_{22} &= f_{22} + f_{23}e_{12} + f_{24}e_{22}, \end{aligned}$$

where

$$(B.2) \qquad \begin{aligned} e_{11} &= \frac{2}{D}(\beta^2 - 1), \quad e_{12} = \frac{\beta - 1}{D}(3\beta + 1.5), \\ e_{21} &= \frac{-\beta + 1}{D}(3\beta^2 - 1.5), \\ e_{22} &= -\frac{1}{D}[(2\beta^2 - 1)(\beta + 0.5) + (2\beta + 1)(\beta - 0.5)], \\ D &= (\beta - 1)(0.5 - \beta), \end{aligned}$$

$$(B.3) \qquad f_{1j} = \frac{f'_{1j}}{\beta + 1}, \quad f_{2j} = \frac{f'_{2j}}{\beta + 0.5}, \quad j = 1, \ldots, 4,$$

and

$$
\begin{aligned}
f'_{11} &= -N_{40}S - \sigma_T N_{30}N_{30} + \sigma_H(-8N_{10}N_{30} - 2N_{30}^2),\\
f'_{12} &= N_{30}S + 2\sigma_T N_{20}N_{40} + \sigma_H(12N_{20}^2 + 4N_{20}N_{40}),\\
f'_{13} &= N_{20}S - 2\sigma_T N_{10}N_{30} + \sigma_H(-4N_{10}N_{30}),\\
f'_{14} &= -N_{10}S + 2\sigma_T N_{20}N_{20} + 2\sigma_H N_{20}^2,\\
f'_{21} &= \sigma_T N_{30}N_{30} + \frac{N_{40}S}{2} + \sigma_H(6N_{10}N_{30} + 2N_{30}^2),\\
f'_{22} &= -2\sigma_T N_{20}N_{40} - \frac{N_{30}S}{2} + \sigma_H(-9N_{20}^2 - 4N_{20}N_{40} - N_{20}^2),\\
f'_{23} &= 2\sigma_T N_{10}N_{30} - \frac{N_{20}S}{2} + \sigma_H(3N_{10}^2 + 4N_{10}N_{30} + 3N_{30}^2),\\
f'_{24} &= -\sigma_T N_{20}N_{20} + \frac{N_{10}S}{2} + \sigma_H(2N_{20}^2 - N_{20}N_{40}),
\end{aligned}
\tag{B.4}
$$

$$
S = 1 + 2\sigma_P N^0, \quad N^0 = N_{10} + \ldots N_{60}, \tag{B.5}
$$

where N^0 is the total density of the equilibrium state, and for simplicity the formulas are reported for the case without the quadruple collisions.

Acknowledgements

The author thanks dr P. CHAUVAT and dr K. PIECHÓR for a useful discussion. The work has been supported by the French Ministry of Research and Technology, and the Polish Government grant CPBP 0102.

References

1. N. BELLOMO and E. LONGO, in: Waves and Stability in Continuous Media [Ed.] S. RIONERO, Worlds Sci., London, Singapore 1991.
2. J. E. BROADWELL, Phys. Fluids, 7, 1243, 1964.
3. P. CHAUVAT, F. COULOUVRAT and R. GATIGNOL, Adv. Kinetic Theory Cont. Mech., [Ed.] E. GATIGNOL, Soubbaramayer, Springer-Verlag, 139, 1991.
4. H. CORNILLE, J. Mat. Phys., 29, 7, 1667, 1988.
5. H. CORNILLE and T. PŁATKOWSKI, submitted to J. Phys. A.
6. U. FRISCH, B. HASSLACHER, Y. POMEAU, Phys. Rev. Letters, 56, 1505, 1986.
7. U. FRISCH, D'HUMIERES, B. HASSLACHER, P. LALLEMAND, Y. POMEAU and J. P. RIVET, Complex Systems 1, 694, 1987.
8. R. GATIGNOL, Lect. Notes in Physics, Springer-Verlag, Berlin 1975.
9. R. GATIGNOL, Proc. 17th RGD, RWTH Aachen, [Ed.] R. BEYLICH, 1990.
10. S. HARRIS, Phys. Fluids, 9, 7, 1328, 1966.
11. S. HARRIS, J. Math. Phys., 8, 12, 2407, 1967.
12. E. LONGO and R. MONACO, Proc. 16th RGD, in: Progr. Astron. Aeron. AAIA, [Ed.] E. MUNTZ, 118, 118, 1989.
13. T. PŁATKOWSKI, Mech. Res. Comm., 11, 3, 201, 1984.
14. T. PŁATKOWSKI, Transp, Th. Stat. Phys., 18, 2, 221, 1989.
15. T. PŁATKOWSKI, in preparation.

UNIVERSITY OF WARSAW
DEPARTMENT OF MATHEMATICS, INFORMATICS AND MECHANICS, WARSZAWA.

Received April 2, 1992.